Supporting Information

Magnetic plasmons induced in a dielectric-metal heterostructure by optical magnetism

Shulei Li,[1] Lidan Zhou,[1,2] Mingcheng Panmai,[1] Jin Xiang [3] and Sheng Lan[1,]*

[1] Guangdong Provincial Key Laboratory of Nanophotonic Functional Materials and Devices, School of Information and Optoelectronic Science and Engineering, South China Normal University, China

[2] State Key Laboratory of Optoelectronic Materials and Technologies and School of Electronics and Information Technology, Sun Yat-sen University, China

[3] Department of Electrical and Computer Engineering, University of Wisconsin–Madison, USA

Corresponding Author:

E-mail : slan@scnu.edu.cn

Supplementary Note 1: Optical properties of TE waves excited in dielectric-metal heterostructures

In order to gain a deep insight into the TE waves excited in Si_3N_4/Ag heterostructures, we calculated the reflection spectra of Si_3N_4/Ag heterostructures with different thicknesses of the Si_3N_4 layer, as shown in Figure S1A. In this case, the incidence angle of the *s*-polarized light was set to be $\theta = 45°$. It is found that a reflection dip with a linewidth of 24 nm, which reflects the excitation of a TE wave in the Si_3N_4/Ag heterostructure, appears at ~420 nm for $d = 40$ nm. With increasing thickness of the Si_3N_4 layer, a red shift of the reflection dip as well as a broadening of the linewidth is observed. When the thickness is increased to $d = 100$ nm, a reflection dip with a linewidth of ~12 nm is observed at ~775 nm. This behavior indicates that the resonant wavelength of the TE wave excited in the Si_3N_4/Ag heterostructure can be varied by changing the thickness of the Si_3N_4 layer. In order to show the sensitivity of the resonant wavelength of the TE wave on the thickness of the Si_3N_4 layer, we calculated the reflection spectra for Si_3N_4/Ag heterostructures whose thickness ranging from $d = 50$ to 51 nm, as shown in Figure S1B. A redshift of the reflection dip with increasing thickness of the Si_3N_4 layer can be clearly discriminated for an increment as small as 1.0 nm. This unique feature of the TE wave can be exploited to build highly sensitive sensors for monitoring the thickness variation of the Si_3N_4 layer, as demonstrated in this work. Apart from the thickness of the Si_3N_4 layer, the resonant wavelength of the TE wave also exhibits strong dependence on the refractive index of the dielectric material, which is used to construct the dielectric-metal heterostructure. In Figure S1C, we show the reflection spectra of dielectric-metal (Ag) heterostructures constructed by using dielectric materials with different refractive indices. Here, the thickness of the dielectric layer was chosen to be $d = 100$ nm and the angle of the *s*-polarized light was set to be $\theta = 45°$. For a dielectric layer with $n = 1.5$, a reflection dip with a linewidth of ~15 nm is found at ~470 nm. A redshift of the reflection dip as well as a narrowing of the linewidth is observed when the refractive index of the dielectric layer is increased. We also examined the sensitivity of the resonant wavelength of the TE wave on the refractive index of the dielectric layer, as shown in Figure S1D. It is found that the resonant wavelength of the TE wave is quite sensitive to the refractive index change of the dielectric layer. A refractive index change as small as Δn ~0.001 can be resolved as a shift of the reflection dip by ~ 1 nm, implying the potential applications in building highly sensitive sensors for detecting the refractive index change. Similar to the TM wave excited on the surface of the metal film, the TE wave excited in the dielectric-metal heterostructure also exhibits a strong dependence on the incidence angle of the *s*-polarized light, as shown in Figure S1E where the reflection spectra of a Si_3N_4/Ag heterostructures with $d = 100$ nm obtained at different incidence angles are presented. This behavior implies that the resonant wavelength of the TE wave can be manipulated by simply varying the incidence

angle of the *s*-polarized light. A detailed scanning of the incidence angle reveals that a small variation of the incidence angle of only 0.1° can be easily identified by the shift of the reflection dip, as shown in Figure S1F.
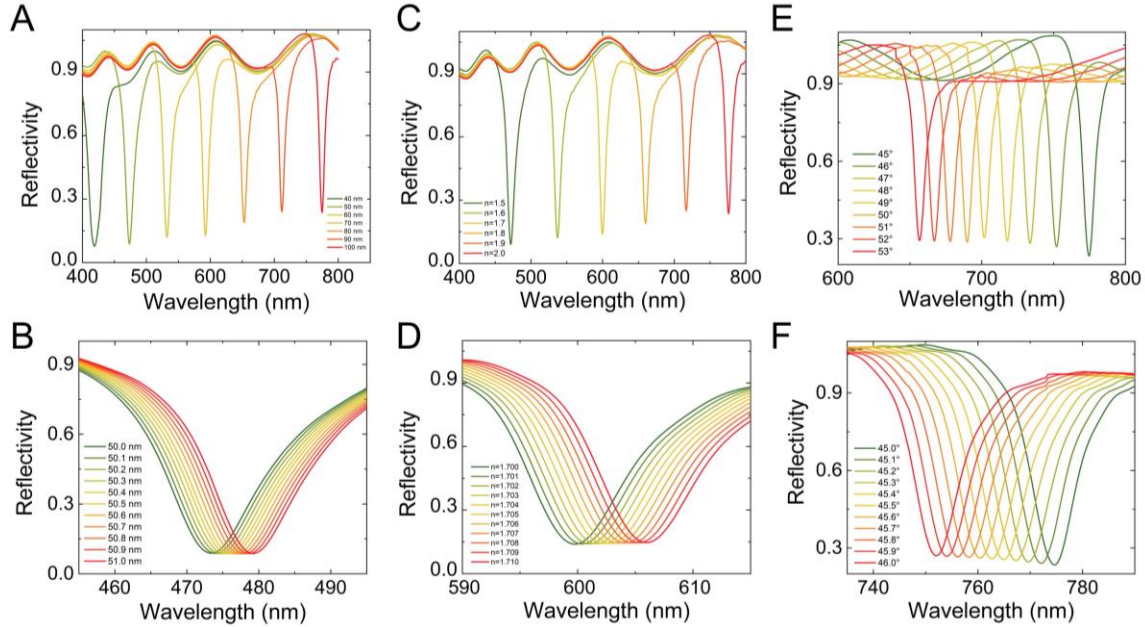
Figure S1 Reflection spectra calculated for the dielectric/Ag heterostructures with different thicknesses of the dielectric (Si_3N_4) layer (A,B), with different refractive indices of the dielectric layer (C,D), and excited by using *s*-polarized light with different incidence angles (E,F).

Supplementary Note 2: Optical properties of a Si_3N_4/Ag heterostructure with a Si_3N_4 layer of $d = 400$ nm

We also examined a Si_3N_4/Ag heterostructure with a thicker Si_3N_4 layer ($d = 400$ nm). In this case, the calculated reflective spectrum is shown in Figure S2A where three reflection dips with narrow linewidths of ~4 nm are observed. They correspond to the first-, second-, and third-order TE waves excited in the Si_3N_4/Ag heterostructure, which simultaneously appearing in the visible light spectrum. In Figure S2B, we show the electric field distribution along the surface normal calculated for the third-order TE wave. A field enhancement factor of ~6.0 is observed. In addition, one can see two nodes of the electric field in the Si_3N_4 layer, corresponding to the order of the TE wave. Finally, the electric field decays rapidly into the Ag film and slowly into air.
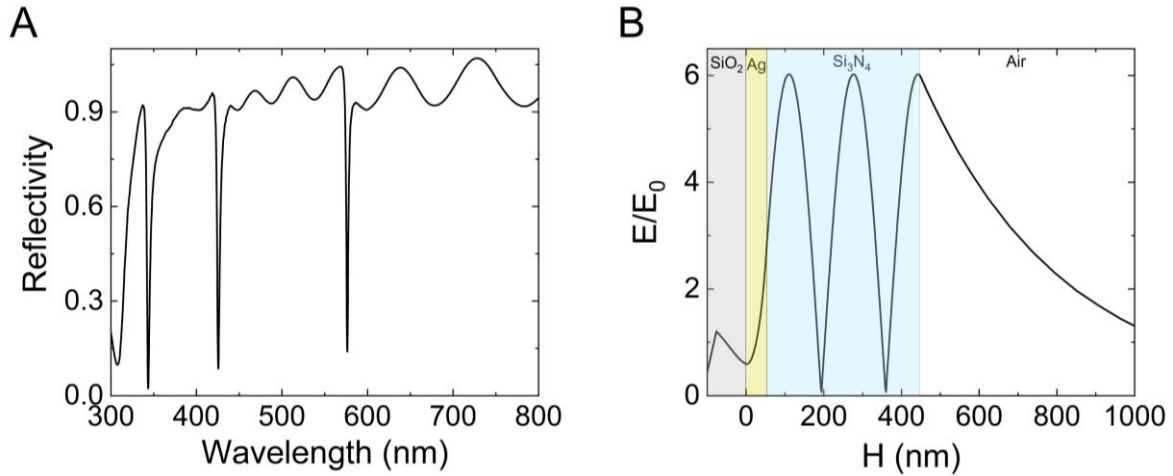
Figure S2 (A) Reflection spectrum calculated for a Si_3N_4/Ag heterostructure with $d = 400$ nm by using s-polarized light at $\theta = 45°$. **(B)** Electric field distribution calculated for a Si_3N_4/Ag heterostructure along the surface normal.

Supplementary Note 3: Optical properties of TM waves excited in dielectric-metal heterostructures

As discussed in the main text, TM waves can be generated on the surface of a bare metal film, which is generally referred to as surface plasmon polaritons (SPPs). This can be considered as a special case for dielectric-metal heterostructures (i.e., air-metal heterostructure). Alternatively, the SPPs can be regard as the lowest-order TM wave of a dielectric-metal heterostructure. In Figure S3A, we show the thickness dispersion relations calculated for Si_3N_4/Ag heterostructures with different thicknesses of the Si_3N_4 layer. It is noticed that the second-order TM wave emerges at ~300 nm when the thickness of the Si_3N_4 layer is increased to ~70 nm. Similarly, the third-order TM wave appears when the thickness is larger than 150 nm. More high-order TM waves enter into the visible light spectrum with increasing thickness of the Si_3N_4 layer. In order to gain a deep insight into the lowest-order TM wave, we calculated the thickness dispersion relation of a Si_3N_4/Ag heterostructure, as shown in Figure S3B. In this case, the incidence angle was chosen to be $\theta = 45°$. It is remarkable that the conventional SPPs are excited at ~650 nm with a broad linewidth of ~70 nm. A redshift of the resonant wavelength is observed with increasing thickness of the Si_3N_4 layer and it becomes larger than 800 nm for $d > 6.0$ nm. The similar phenomenon is observed in the refractive index dispersion relation calculated for dielectric/Ag heterostructures with different refractive indices of the dielectric layer, as shown in Figure S3C. For $n > 1.5$, the second-order TM wave begins to enter into the visible light spectrum. A dielectric layer with $n > 2.5$ is necessary in order to see the third-order TM wave in the visible light spectrum. In Figure S3D, we show the refractive index dispersion calculated for the lowest-order TM wave. Similarly, one can see a redshift of the resonant

wavelength from ~650 to ~800 nm when the refractive index of the dielectric layer is changed from n = 1.00 to n = 1.02. In Figure S3E, we present the dependence of the resonant wavelength of the first-order TM wave on the incidence angle. A strong dependence of the resonant wavelength on the incidence angle is observed for $44° < \theta < 50°$. For $\theta > 55°$, the resonant wavelength becomes not sensitive to the incidence angle.
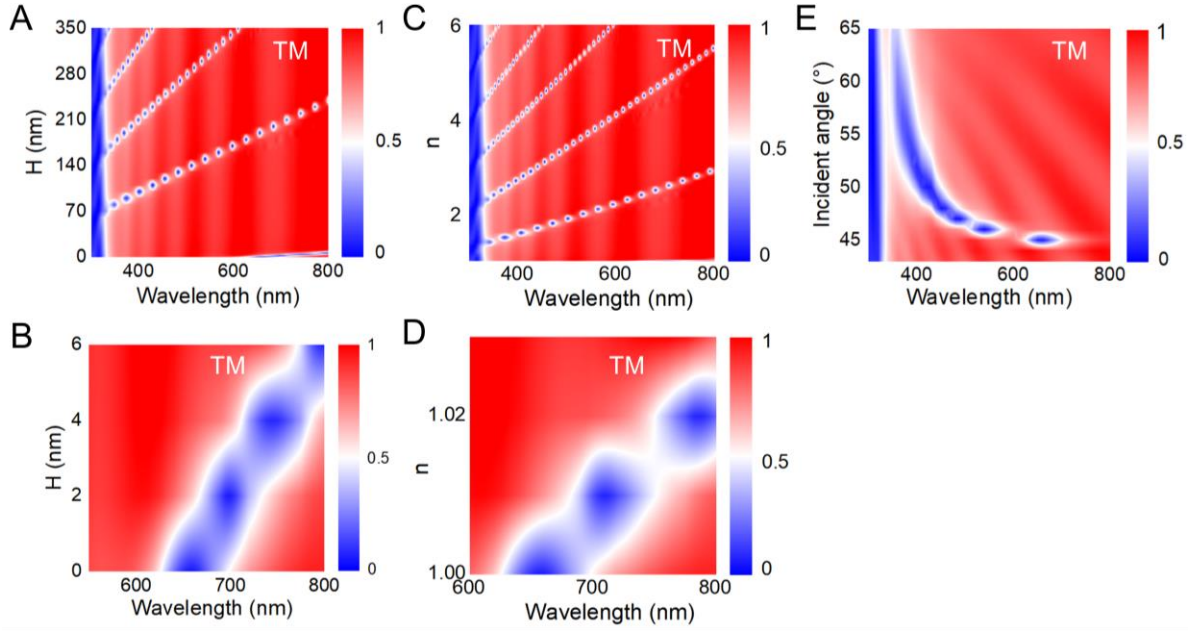

Figure S3 (A) Thickness dispersion relations calculated for TM waves of different orders. (B) Thickness dispersion relation calculated for the TM wave of the lowest order. (C) Refractive index dispersion relations calculated for TM waves of different orders. (D) Refractive index dispersion relation calculated for the TM wave of the lowest order. (E) Dependence of the resonant wavelength of the lowest-order TM wave on the incidence angle of the *p*-polarized light.

Supplementary Note 4: Optical properties of the second-order TM wave excited in dielectric-metal heterostructures (simulation)

Similar to the lowest-order TE wave, we also examined the optical properties of the second-order TM wave excited in dielectric-metal heterostructures, including the thickness and refractive index dependences. We first calculated the reflection spectra of Si_3N_4/Ag heterostructures with different thicknesses of the Si_3N_4 layer, as shown in Figure S4A. In this case, the incidence angle of the *p*-polarized light was set to be $\theta = 45°$. It is found that a reflection dip with a linewidth of ~14 nm, which reflects the

excitation of a TM wave in the Si_3N_4/Ag heterostructure, appears at ~420 nm for d = 110 nm. With increasing thickness of the Si_3N_4 layer, a red shift of the reflection dip as well as a broadening of the linewidth is observed. When the thickness is increased to d = 210 nm, a reflection dip with a linewidth of ~10 nm is observed at ~713 nm. This behavior indicates that the resonant wavelength of the TM wave excited in the Si_3N_4/Ag heterostructure can be varied by changing the thickness of the Si_3N_4 layer. In order to show the sensitivity of the resonant wavelength of the TM wave on the thickness of the Si_3N_4 layer, we calculated the reflection spectra of Si_3N_4/Ag heterostructures with thickness ranging from d = 150 to 151 nm, as shown in Figure S4B. A redshift of the reflection dip with increasing thickness of the Si_3N_4 layer can be clearly discriminated for an increment as small as 0.3 nm. This unique feature of the TM wave can be exploited to build highly sensitive sensors for monitoring the thickness variation of the Si_3N_4 layer, as demonstrated in this work. Apart from the thickness of the Si_3N_4 layer, the resonant wavelength of the TM wave also exhibits strong dependence on the refractive index of the dielectric material, which is used to construct the dielectric-metal heterostructure. In Figure S4C, we show the reflection spectra of dielectric-metal heterostructures constructed by using dielectric materials with different refractive indices. Here, the thickness of the dielectric layer was chosen to be d = 150 nm and the angle of the p-polarized light was set to be θ = 45°. For a dielectric layer with n = 1.6, a reflection dip with a linewidth of ~17 nm is found at ~405 nm. A redshift of the reflection dip as well as a narrowing of the linewidth is observed when the refractive index of the dielectric layer is increased. We also examined the sensitivity of the resonant wavelength of the TM wave on the refractive index of the dielectric layer, as shown in Figure S4D. It is found that the resonant wavelength of the TM wave is quite sensitive to the refractive index change of the dielectric layer. A refractive index change as small as Δn ~0.001 can be resolved as a shift of the reflection dip by ~ 0.6 nm, implying the potential applications in building highly sensitive sensors for detecting the refractive index change. Similar to the TE wave excited on the surface of the metal film, the TM wave excited in the dielectric-metal heterostructures also exhibits a strong dependence on the incidence angle of the p-polarized light, as shown in Figure S4E where the reflection spectra of a Si_3N_4/Ag heterostructure with d = 0 nm obtained at different incidence angles are presented.
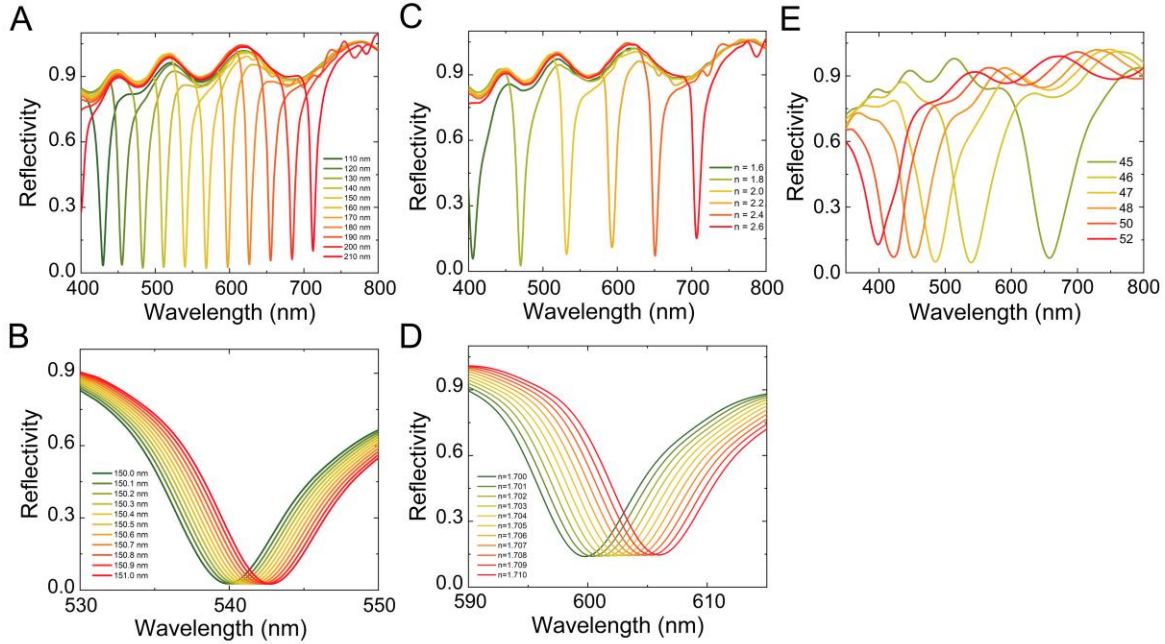
Figure S4 Reflection spectra calculated for the dielectric/Ag heterostructures with different thicknesses of the dielectric (Si$_3$N$_4$) layer (A,B), with different refractive indices of the dielectric layer (C,D), and excited by using *p*-polarized light with different incidence angles (E).

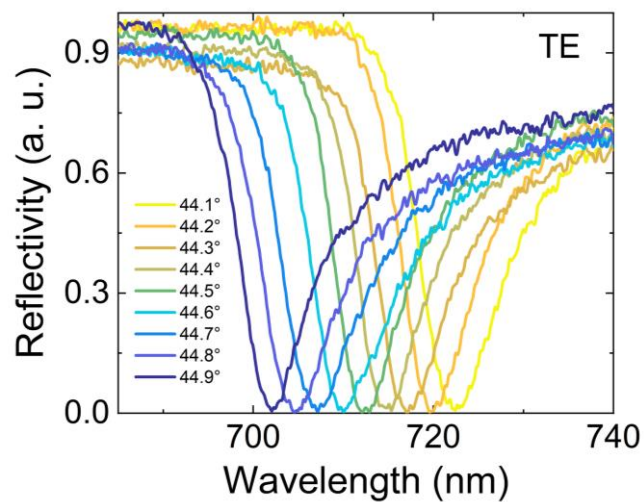## Supplementary Note 5: Tuning the resonant wavelength of the second-order TM wave by varying the incidence angle

We also examined the dependence of the resonant wavelength of the second-order TM wave excited in the Si$_3$N$_4$/Ag heterostructure on the incidence angle of the *p*-polarized light, as shown in Figure S5A. With increasing the incidence angle, a blueshift of the resonant wavelength is observed. This behavior implies that the resonant wavelength of the TM wave can be manipulated by simply varying the incidence angle of the *p*-polarized light. A detailed scanning of the incidence angle reveals that a small variation of the incidence angle of only 0.1° can be easily identified by the shift of the reflection dip, as shown in Figure S5B.
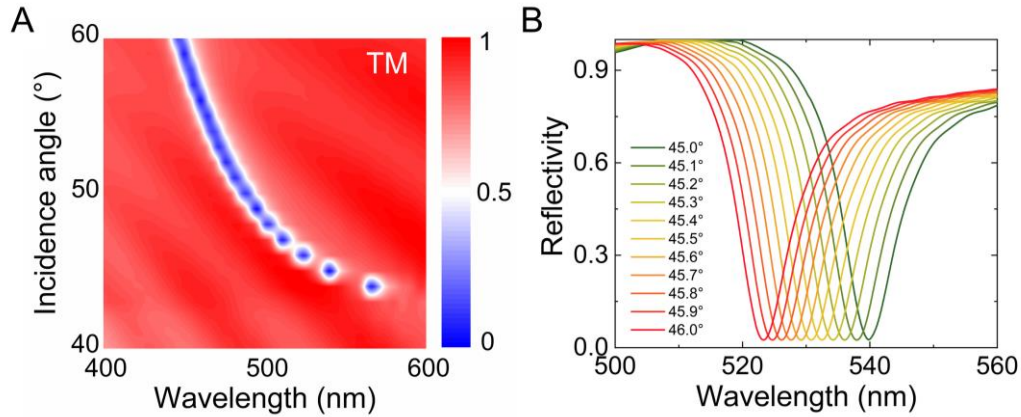
Figure S5 (A) Dependence of the resonant wavelength of the second-order TM wave on the incidence angle of the *p*-polarized light. (B) Reflection spectra of the second-order TM waves excited by using p-polarized at different incidence angles.

Supplementary Note 6: Reflection spectra measured for a Si₃N₄/Ag heterostructure excited by TE wave

We also measured the reflection spectra of a Si_3N_4/Ag heterostructure with $d = 100$ nm excited by using *s*-polarized light at different incidence angles ranging from 44.1° to 44.9°, as shown in Figure S6. As expected, the large blueshift and narrow linewidth of the reflection dip makes it possible to discriminate the incidence angle change as small as 0.1°.


Figure S6 Dependence of the resonant wavelength of the TE wave on the incidence angle of the *s*-polarized light.

Supplementary Note 7: Optical properties of the second-order TM wave excited in dielectric-metal heterostructures (experiment)

We examined the optical properties of the second-order TM wave excited in a Si_3N_4/Ag heterostructure (d = 200 nm) by using p-polarized light at different incidence angles. In Figure S7A, we show the reflection spectra obtained for the heterostructure at different incidence angles. As expected, the reflection dip can be shifted from 640 to 550 nm when the incidence angle is increased from 44° to 49°. A detailed scanning of the incidence angle reveals that a small variation of the incidence angle of only 0.2° can be easily identified by the shift of the reflection dip, as shown in Figure S7B. In practical applications, the use of scattered light is more convenient than the reflected light. For this reason, we also examined the scattering spectra of a PS nanosphere with a diameter of D = 300 nm placed on the heterostructure, as shown in Figure S7C. In this case, a blueshift of the scattering peak from ~610 to 500 nm, which is correlated with the TM wave generated in the heterostructure, is achieved when the incidence angle is increased from 44° to 58°, spanning the whole visible light spectrum. In Figure S7D, we present the color indices of the scattering light extracted from the scattering spectra of the PS nanosphere. It can be seen that they are distributed outside the RGB triangle, implying the good chromaticity of the scattering light. It implies the potential application of the TM wave in nanoscale optical display, as shown in Figure S7E where the scattering light with vivid color recorded by using a charge-coupled device is presented.
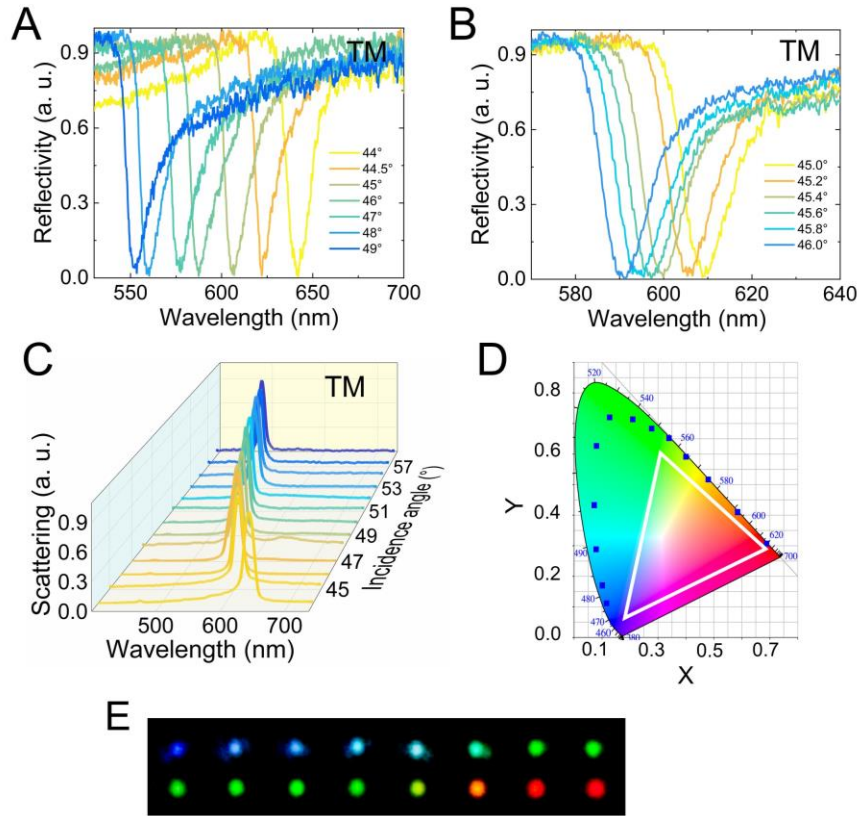
Figure S7 (A,B) Reflection spectra measured for a Si₃N₄/Ag heterostructure (d = 200 nm) excited by using p-polarized at different incidence angles. (C) Scattering spectra measured for a PS nanosphere with D = 300 nm excited by using the TM wave generated on the surface of a Si₃N₄/Ag heterostructure by using p-polarized at different incidence angles. (D) Colour indices extracted from the scattering spectra of the PS nanosphere shown in (C). (E) CCD images of the scattering light measured the TM waves excited at different incidence angles.

Supplementary Note 8: Scattering of TE waves by nanoholes made in dielectric-metal heterostructures

In order to demonstrate the applications of the TE waves excited in dielectric-metal heterostructures in high-quality color display, we made nanoholes in a Si₃N₄/Ag heterostructure to show SCNU, which is the abbreviation of our university, as shown in Figure S8A where the scanning electron microscope (SEM) image of the fabricated pattern and the constituent nanoholes are presented. In Figure S8B, we show the images of the SCNU pattern illuminated by using the TE waves generated in the heterostructure with s-polarized light at different incidence angles. It is found that patterns decorated with green, yellow, orange, and red colors can be achieved by simply varying the incidence angle.
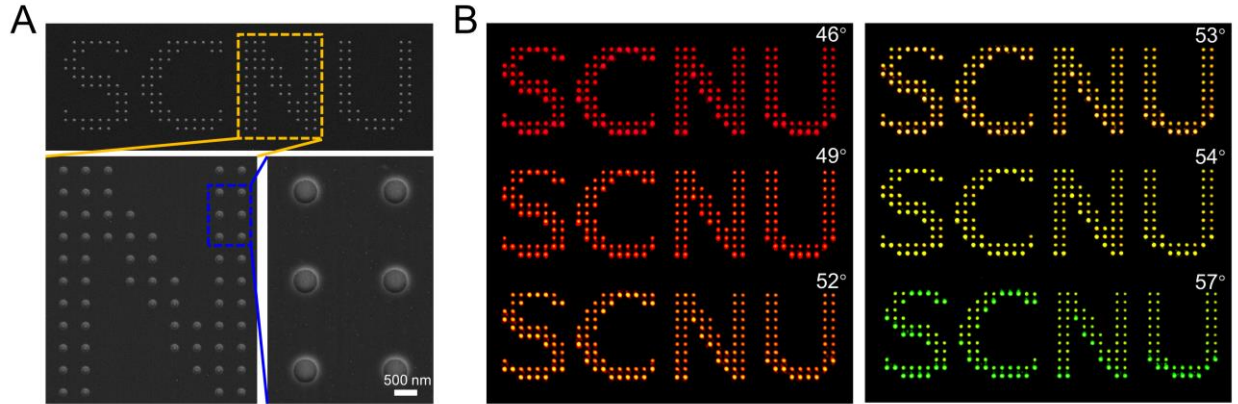
Figure S8 (A) SEM image of the nanoholes made in the Si_3N_4 layer of a Si_3N_4/Ag heterostructure. (B) Images of SCNU pattern illuminated by using the TE waves generated in the Si_3N_4/Ag heterostructure at different incidence angles.

Supplementary Note 9: Sensing the evaporation of alcohol

Here, we demonstrated a highly sensitive optical sensing by exploiting the unique feature of the TE waves. In experiments, we covered the surface of the Si_3N_4/Ag sample with patterned nanoholes with a thin alcohol film on by using spin-coating. The reason for choosing alcohol is due to the rapid evaporation of alcohol in air and the large expansion coefficient of alcohol upon heating. These two features were employed to change the thickness of the thin alcohol film. In this case, the resonant wavelength of the TE wave at a specified incidence angle was dictated by the effective thickness of the dielectric layer, which is now the Si_3N_4 layer plus the alcohol film. If we monitored the scattering peak of a nanohole for the TE wave excited at $\theta = 48°$, a gradual blueshift was seen with increasing observation time, as shown in Figure S9A,B. This blueshift was caused by the gradual evaporation of alcohol in air, which reduces the effective thickness of the dielectric layer. A blueshift of ~5.0 nm was found in the scattering peak after ~300 s, which implies a reduction of ~7.5 nm in the thickness of the alcohol film due to evaporation.
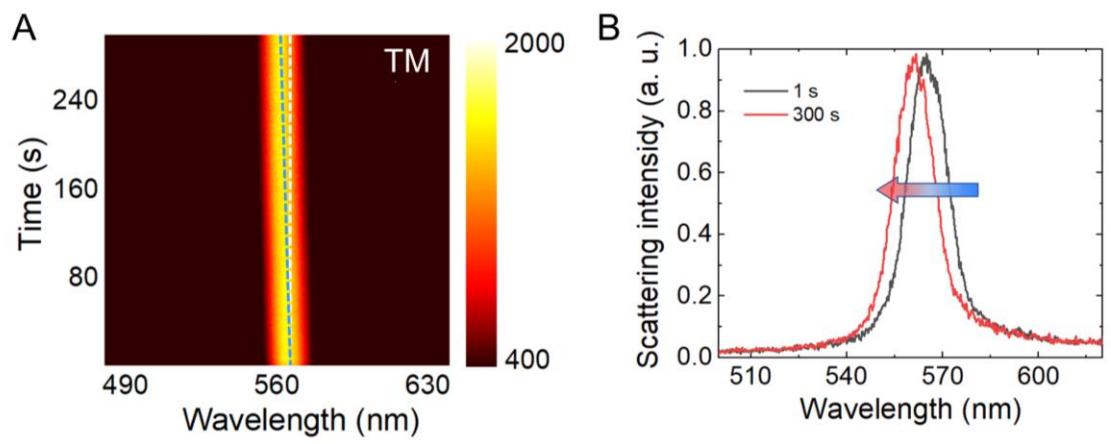
Figure S9 (A) Temporal evolution of the scattering spectrum of a nanohole made in a Si₃N₄/Ag heterostructures excited by *s*-polarized light. (B) Scattering spectrum of the nanohole obtained at different times of *t* = 1.0 and 300 s.